



Characterization of a new natural fiber from *Arundo donax* L. as potential reinforcement of polymer composites



V. Fiore*, T. Scalici, A. Valenza

Department of "Ingegneria Civile, Ambientale, Aerospaziale, dei Materiali", University of Palermo, 90128 Palermo, Italy

ARTICLE INFO

Article history:

Received 11 December 2013

Received in revised form 24 January 2014

Accepted 5 February 2014

Available online 14 February 2014

Keywords:

Arundo donax fiber

Mechanical property

Infrared spectroscopy

Thermogravimetric analysis

Scanning electron microscopy

Statistical analysis

ABSTRACT

The aim of this paper is to study the possibility of using of *Arundo donax* L. fibers as reinforcement in polymer composites. The fibers are extracted from the outer part of the stem of the plant, which widely grows in Mediterranean area and is diffused all around the world. To use these lignocellulosic fibers as reinforcement in polymer composites, it is necessary to investigate their microstructure, chemical composition and mechanical properties.

Therefore, the morphology of *A. donax* L. fibers was investigated through electron microscopy, the thermal behavior through thermogravimetric analysis and the real density through a helium pycnometer. The chemical composition of the natural fibers in terms of cellulose, hemicellulose, lignin, and ash contents was determined by using standard test methods.

The mechanical characterization was carried out through single fiber tensile tests and a reliability analysis of the experimental data was performed. Furthermore, a mathematical model was applied to investigate the relation between the transverse dimension of the fibers and the mechanical properties.

© 2014 Elsevier Ltd. All rights reserved.

1. Introduction

Over the last decade, a growing attention on the use of natural fibers instead synthetic ones (i.e. glass, carbon or kevlar fibers) has been focused by both the academic world and several industries. The main reasons of this interest are related to the specific properties, price and low environmental impact of this kind of fibers. A great variety of different natural fibers are actually available as reinforcements of polymer composites. The most widely used are flax, hemp, jute, kenaf and sisal, because of their properties and availability. Some recent scientific works advance the feasibility to use less common natural fibers, such like artichoke (Fiore, Valenza, & Di Bella, 2011), okra (De Rosa, Kenny, Puglia, Santulli, & Sarasini, 2010), isora (Mathew, Joseph, & Joseph, 2006), ferula (Seki, Sarikanat, Sever, & Durmuşkahya, 2013), althaea (Sarikanat, Seki, Sever, & Durmuşkahya, 2014), piassava (d'Almeida, Aquino, & Monteiro, 2006), sansevieria (Sathishkumar, Navaneethakrishnan, Shankar, & Rajasekar, 2013) and buriti (da Silva Santos, de Souza, De Paoli, & de Souza, 2010) as reinforcement for composite materials. In this work, a new kind of fibers, extracted from the stem of the giant reed *Arundo donax* L., is investigated as a potential

reinforcement in polymer composites. The giant reed is a perennial rhizomatous grass that grows plenty and naturally in all the temperate areas of Europe (mainly in the countries of the Mediterranean area as Sicily) and can be easily adapted to different climatic conditions. Thanks to its high growth rate, it represents an invasive and aggressive species so its disposal is difficult. Its field of application is very wide, ranging from the production of reeds in musical woodwind instruments for at least 5000 years to the use as a source of fibers for printing paper (Ververis, Georgiou, Christodoulakis, Santas, & Santas, 2004). *A. donax* L. is also used as a diuretic and as a source of biomass for chemical feedstocks and for energy production. Furthermore, this non-wood plant is recently considered in the manufacturing of chipboard panels alternative to those wood-based ones (Flores, Pastor, Martinez-Gabaron, Gimeno-Blanes, & Rodriguez-Guisado, 2011). The stem of the giant reed is often used to make fences, trellises, stakes for plants, windbreaks, sun shelters (Pilu, Bucci, Badone, & Landoni, 2012). Owing to their specific mechanical properties (e.g. strength–density ratio), the stems of the giant reed are also employed in agricultural building. These fibers have been chosen for several reasons:

1. It is a non-wood plant that grows plenty and naturally in Sicily. Thanks to its high growth rate, it represents an invasive and aggressive species so its disposal is difficult.

* Corresponding author. Tel.: +39 091 23863721; fax: +39 091 7025020.
E-mail address: vincenzo.fiore@unipa.it (V. Fiore).



Fig. 1. Arundo fibers isolated from the stem.

2. As shown previously, the *A. donax* L. is used for many applications: it is source of biomass and it is used as raw material in music instruments industry. It is also a source of cellulose for paper industry and it has an important role in reinforcement of riverbanks and soil in wetlands.
3. It is widely diffused all around the world. The adaptability and high growth rate of this plant could allow to access to big reserves of raw material.

The idea of the authors is to collect these plants in order to extract fibers from outer part of the stem and verifying the possibility to use them as reinforcement of polymer composites.

2. Materials and methods

A. donax L. has been collected after flowering in a plantation in the area of Palermo (Sicily). After collecting the fresh plant, the stem, having outer and inner average diameters equal to 25 mm and 17 mm, was separated from the foliage. Then, the stem was cut into small parts and dried at 103 °C for 24 h in an oven to remove all the moisture content, according to ASABE S358.3 (2012).

After this phase, the fibers with a length between 100 mm and 160 mm were extracted from the stem by mechanical separation. In particular, the outer part of the culm was manually decorticated with the help of blades obtaining thin strips from which fibers were easily separated with the aid of a scalpel and a Leica optical microscope model MS5.

The fibers thus obtained, shown in Fig. 1, were kept in moisture-proof container.

Like other natural fibers, those extracted from the stem of arundo plant have a complex, layered structure consisting of a thin primary wall which is the first layer deposited during cell growth encircling a secondary wall. The secondary wall is made up of three layers (named S1, S2 and S3) and the thick middle layer determines the mechanical properties of the fiber. The middle layer consists of a series of helically wound cellular microfibrils formed from long chain cellulose molecules, bounded together by an amorphous lignin matrix; the hemicellulose acts as a compatibilizer between cellulose and lignin (Kalia, Kaith, & Kaur, 2009; Rong, Zhang, Liu, Yang, & Zeng, 2001) while pectin is also a bonding agent. The angle between the fiber axis and the microfibrils is called the microfibril angle α . The characteristic value of microfibril angle varies from one fiber to another.

As widely known, lignocellulosic fibers show a non-uniform cross section and irregular shape. In this work, the diameter of Arundo fiber was measured through optical observations (Leica optical microscope model MS5) at three different random locations along the single fiber. The apparent cross-sectional area of each

fiber was then calculated from the average fiber diameter assuming a circular cross-section, as suggested by the literature (Silva, Chawla, & Toledo Filho, 2008; De Rosa et al., 2010).

The real density of arundo fibers was measured using gas intrusion under helium gas flow with a Pycnomatic ATC Thermo Electron Corporation equipment pycnometer. Five measurements were conducted at 20 °C. The cellulose content of arundo fibers was calculated by means of the density method suggested by Mwaikambo and Ansell (2001). This method allows to determine the cellulose content by measuring the real (with the technique of helium pycnometry) and apparent density (with the Archimedes method using benzene as a solvent) of arundo fibers.

In particular, benzene with a density of 0.875 g/cm³ was used as a non polar solvent for the measurement of the bulk density of fibers and an electronic balance was used to weigh fibers. A sample of fibers was first weighted in air and then immersed in benzene solvent and reweighted. The apparent density ρ_A of the fibers was calculated using the following equation:

$$\rho_A = \frac{\rho_s \cdot W_{fa}}{W_{fa} - W_{fb}} \quad (1)$$

where ρ_s is the density of benzene; W_{fa} and W_{fb} are the weights of the fibers in air and in benzene, respectively.

The indirect calculation of the cellulose content of arundo fibers can be performed using the following equation, as suggested by Mwaikambo and Ansell (2001):

$$\%cell = \left[2 \cdot \left(\frac{\rho_a}{\rho_r} + \frac{\rho_r}{\rho_{cell}} \right) - \frac{\rho_a}{\rho_{cell}} - 2 \right] \cdot 100 \quad (2)$$

where $\rho_{cell} = 1.592$ g/cm³ (density of cellulose) (Meredith, 1956).

Thermogravimetric analysis (TGA) was carried out to define the thermal stability of arundo fibers by using a thermobalance TG/DTA Perkin Elmer 6000. Particularly, samples of weights between 2 and 5 mg were placed in an alumina pan and heated from 30 to 750 °C at a heating rate of 10 °C/min in air atmosphere. The microstructure and morphology of the fiber were investigated by scanning electron microscopy (SEM) using a FEI QUANTA 200 F. Before analysis, each fiber was cut to a height of 10 mm, coated with gold and rubbed upon a 25 mm diameter aluminum disc. Fourier transform infrared spectrometry (FTIR) was carried out on arundo fibers to analyze the chemical structure of their components. IR spectrum of the fibers was recorded at the resolutions of 1 cm⁻¹ using a Perkin Elmer spectrometer in the frequency range 4000–500 cm⁻¹, operating in attenuated total reflectance (ATR) mode. Forty fibers were mechanically tested in tension, according to ASTM D3379–75 standards, using an UTM by Zwick-Roell, equipped with a load cell of 200 N, at a constant strain rate of 1 mm/min and gage length of 30 mm. The results were analyzed statistically using an ad-hoc code developed in Matlab® environment, as suggested in the literature about the mechanical tests of natural fibers.

3. Results and discussion

3.1. Real density and chemical composition

The real density ρ_r of arundo fibers, measured using a helium pycnometer, is 1.168 ± 0.003 g/cm³. The bulk density of arundo fibers, measured following the procedure described in Section 2, is 0.893 g/cm³.

The obtained value of cellulose content of arundo fibers, calculated using Eq. (2), is equal to 43.59%.

Like other natural fibers, the principal chemical constituents of those extracted from the stem of arundo plant are cellulose, hemicelluloses and lignin. Cellulose is characterized by the least variation in chemical structure and can be considered the major framework component of the fiber.

Cellulose is a strong, linear (crystalline) molecule with no branching. It is the main component providing the strength, stiffness and structural stability. It has good resistance to hydrolysis although all chemical and solution treatments will degrade it to some extent. Hemicelluloses are lower molecular weight polysaccharides, often copolymers of glucose, glucuronic acid, mannose, arabinose and xylose, that form random, amorphous branched or nonlinear structures with low strength. Lignin is an amorphous, cross-linked polymer network consisting of an irregular array of variously bonded hydroxy- and methoxy-substituted phenylpropane units. Its chemical structure varies depending on its source. Lignin is less polar than cellulose and acts as a chemical adhesive both within and between fibers. As lignin becomes more rigid, it places away from the lumen surface and porous wall regions to maintain wall strength and permeability and help with the transport of water. Lignin resists attack by most microorganisms as the aromatic rings are resistant to anaerobic processes while aerobic breakdown of lignin is slow. The mechanical properties are lower than those of cellulose (Di Bella, Fiore, & Valenza, 2012).

To determinate precisely the chemical composition of the natural fibers (i.e. the cellulose, hemicellulose, lignin and ash contents) standard test methods were used. In particular, the hemicellulose content was determined as suggested by literature (Saura-Calixto, Cañellas, & Garcia-Raso, 1983).

The lignin and ash contents were determined according to ASTM D1106–96 and ASTM E1755–01 standards, respectively. The cellulose content in arundo fibers was determined as the Acid Detergent Fiber (ADF) according to AOAC method 973.18. Table 1 (Arrakhiz et al., 2012; Bledzki, Reihmane, & Gassan, 1996; d'Almeida et al., 2006; Das et al., 2000; De Rosa et al., 2010; Fiore et al., 2011; Hornsby, Hinrichsen, & Tarverdi, 1997; John & Anandjiwala, 2008; Li, Mai, & Ye, 2000; Mathew et al., 2006; Mwaikambo & Ansell, 2002; Ouajai & Shanks, 2005; Paiva, Ammar, Campos, Cheikh, & Cunha, 2007; Sarikanat et al., 2014; Seki et al., 2013; Yao, Wu, Lei, Guo, & Xu, 2008) shows the chemical compositions of arundo fiber and other natural fibers.

It is worth note that lignin content of arundo fiber is greater than those of other less common natural fibers (i.e. artichoke, okra, ferula and althaea) and sisal, ramie, jute and flax fibers. Hemicellulose content of arundo fiber is close to those of flax and okra fiber.

The content of cellulose in arundo fiber, compared to those of other fibers, can be considered as relatively low.

3.2. Thermal analysis

The thermal stability of natural fibers can be considered as one of the limiting factors in their use as reinforcement in composite structures (d'Almeida et al., 2006; da Silva Santos et al., 2010; De Rosa et al., 2010; Fiore et al., 2011; Mathew et al., 2006; Sarikanat et al., 2014; Sathishkumar et al., 2013; Seki et al., 2013). The results of the thermogravimetric analysis of arundo fibers are shown in Fig. 2.

The DTG curve of arundo fibers shows an initial peak between 40 and 115 °C (loss in weight about 8%), which corresponds to the vaporization of absorbed water in the fiber. After this peak, the curve exhibits four degradation steps. In particular, thermal degradation of arundo fibers starts at 275 °C (onset degradation temperature) and the first degradation shoulder peak occurs at about 295 °C, is attributed to the thermal depolymerization of hemicelluloses and pectin and the glycosidic linkages of cellulose (12% weight loss). The major second peak, at about 320 °C, is due the degradation of α -cellulose (70% weight loss) (Albano, Gonzalez, Ichazo, & Kaiser, 1999). Similar peaks were observed at 321 °C, 308.2 °C, 298.2 °C and 309.2 °C for bamboo, hemp, jute and kenaf fibers, respectively (Yao et al., 2008). The small third and fourth peaks (at 435 °C and 518 °C and loss in weight equal to 9% and

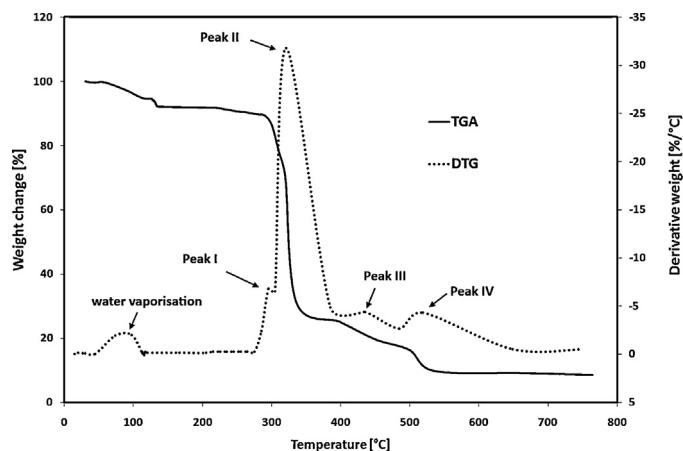


Fig. 2. TG and DTG curves of arundo fibers.

7%, respectively) may be attributed to oxidative degradation of the charred residue (Das et al., 2000). The degradation of lignin, whose structure is a complex composition of aromatic rings with various branches, happens at a very low weight loss rate within the whole temperature range from ambient to temperatures higher to 700 °C (De Rosa et al., 2010; Fiore et al., 2011; Yang, Yan, Chen, Lee, & Zheng, 2007). It is worth note that arundo fibers are stable until around 275 °C. This is in agreement with the values of other natural fibers, as shown in Table 1. So, arundo fibers can be used as reinforcement in composites if molding of thermoset and thermoplastic polymer matrix occurs under this temperature.

3.3. Surface morphology

Fig. 3 shows the surface morphology of arundo fibers. Like other natural fibers the surface morphology of the fiber of arundo consists of several elementary fibers (known as fibrils or fiber-cells) bonded together in the direction of their length by pectin and other non-cellulosic compounds (Arifuzzaman Khan et al., 2009; De Rosa et al., 2010; Fiore et al., 2011) to form a bundle.

The presence of some impurities is also evident on the surface of the fibers, typical of the raw natural fibers. To eliminate these impurities enhancing interfacial adhesion with polymer matrices, natural fibers are often treated chemically (George, Sreekala, & Thomas, 2001; Mohanty, Misra, & Drzal, 2001). Fig. 4(a) shows the cross section of arundo fibers made up of vascular

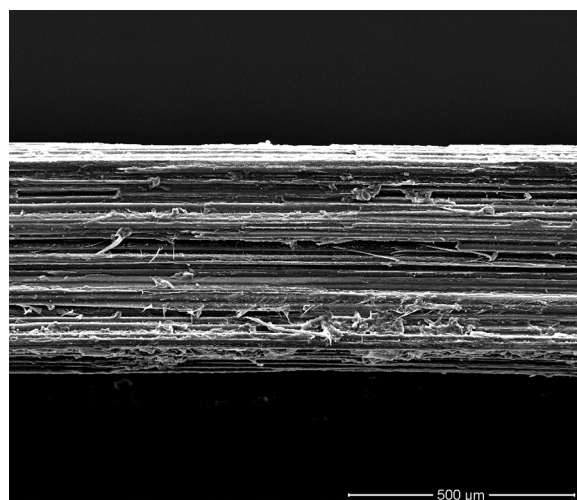


Fig. 3. SEM micrograph of longitudinal view of arundo fibers.

Table 1
Composition and properties of arundo fibers and some natural fibers from literature.

| Fiber | Cellulose [%wt] | Hemicellulose [%wt] | Lignin [%wt] | Ash [%wt] | T_{onset} [°C] | Density [g/cm ³] | Tensile strength [MPa] | Young's modulus [GPa] | Elongation at break [%] |
|-----------|-----------------|---------------------|--------------|-----------|-------------------------|------------------------------|------------------------|-----------------------|-------------------------|
| Artichoke | 75.3 | – | 4.3 | 2.2 | 230 | 1.579 | 201 | 11.6 | – |
| Okra | 60–70 | 15–20 | 5–10 | – | 220 | – | 281 | 16.5 | – |
| Ferula | 53.3 | 8.5 | 1.4 | 7.0 | 200 | 1.24 | 475 | 52.7 | 4.2 |
| Althaea | 44.6 | 13.5 | 2.7 | 2.3 | 220 | 1.18 | 415 | 65.4 | 3.9 |
| Piassava | 31.6 | – | 48.4 | – | 225 | 1.40 | 77 | 2.93 | 10.45 |
| Alfa | 45 | – | 23 | 2 | 320 | 0.89 | 250 | 20 | – |
| Sisal | 78 | 10 | 8 | – | 302 | 1.50 | 511–635 | 9.4–22 | 2–2.5 |
| Coir | 43 | 0.3 | 45 | – | – | 1.20 | 175 | 4–6 | 30 |
| Ramie | 76 | 15 | 1 | – | – | 1.50 | 560 | 24.5 | 2.5 |
| Jute | 72 | 13 | 13 | – | 330 | 1.30 | 393–773 | 26.5 | 1.5–1.8 |
| Flax | 81 | 16.7–20.6 | 3 | – | 282 | 1.50 | 345–1035 | 27.6 | 2.7–3.2 |
| Bamboo | 26–43 | 30 | 21–31 | – | 214 | 0.60–1.10 | 140–230 | 11–17 | – |
| Cotton | 85–90 | 5.7 | – | – | – | 1.50–1.60 | 287–597 | 5.5–12.6 | 7–8 |
| Arundo | 43.2 | 20.5 | 17.2 | 1.9 | 275 | 1.168 | 248 | 9.4 | 3.24 |

bundles and fiber-cells, with polygonal shape and a central hole, named lumen (Silva et al., 2008). In particular, the fiber-cells

structure is highlighted in Fig. 4(b). Like other natural fibers, the

variability in diameter of fiber-cells and lumen has a great influence on the mechanical properties of arundo fibers (De Rosa et al., 2010).

3.4. Fourier transforms infrared spectroscopy

ATR-FTIR assignment of functional groups of arundo fiber can be seen in Fig. 5. The peak at 3400 cm^{-1} can be caused by the O–H stretching vibration and hydrogen bond of the hydroxyl groups (Seki et al., 2013; Yang et al., 2007). The peaks at 2923 cm^{-1} and 2854 cm^{-1} are the characteristic band for the C–H stretching vibration from CH and CH₂ in cellulose and hemicellulose components (Paiva et al., 2007) while the absorption band centered at 1730 cm^{-1} can be attributed to the C=O stretching vibration of the acetyl groups in hemicellulose (Biagiotti et al., 2004).

The peak centered at 1594 cm^{-1} may be explained by the presence of water in the fibers (Olsson & Salmen, 2004) while the little peak at 1506 cm^{-1} is attributed to C=C stretching of benzene ring of the lignin (De Rosa et al., 2010). The absorbance at 1422 cm^{-1} is associated to the CH₂ symmetric bending (Sgriccia, Hawley, & Misra, 2008). The two peaks observed at 1372 cm^{-1} and 1318 cm^{-1} are attributed to the bending vibration of C–H and C–O groups of the aromatic ring in polysaccharides (Le Troedec et al.,

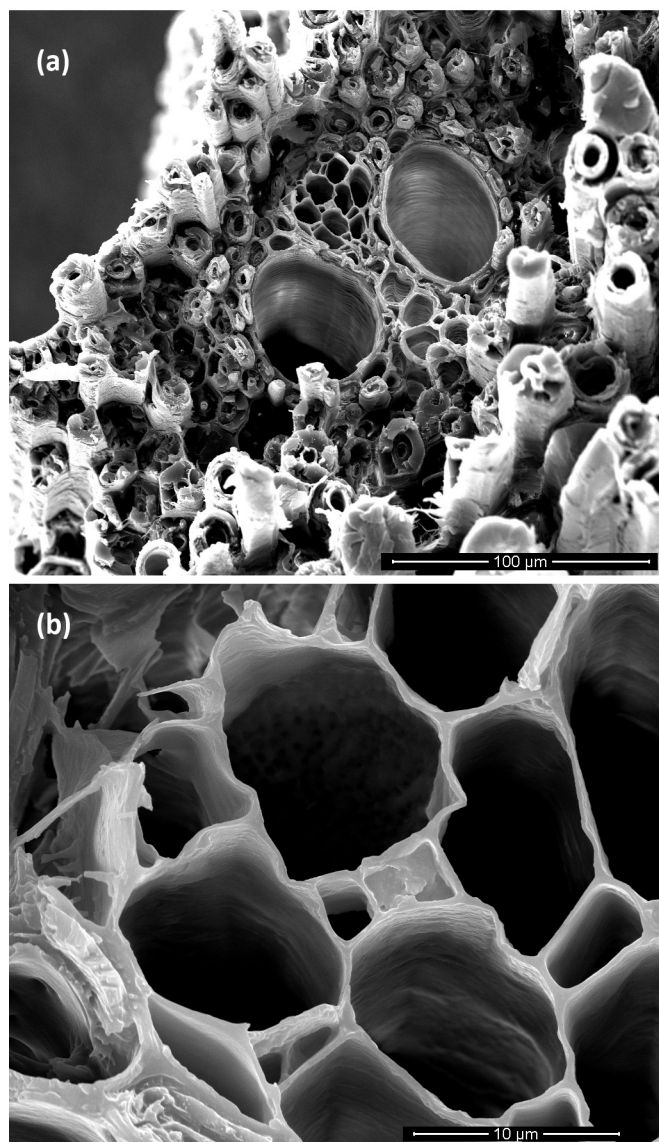


Fig. 4. SEM micrographs of cross section of arundo fibers at two different magnifications: (a) lower and (b) higher.

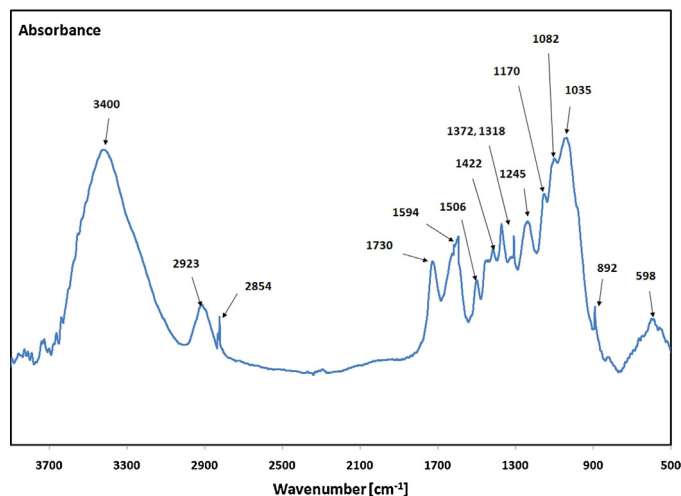


Fig. 5. FTIR spectrum of arundo fibers.

2008) while the absorbance peak centered at 1245 cm^{-1} is due to the C–O stretching vibration of the acetyl group in lignin (Liu, Mohanty, Drzal, Askel, & Misra, 2004). The two peaks at 1170 cm^{-1} and 1082 cm^{-1} are associated to C–O–C stretching vibration of the pyranose ring in polysaccharides (Yang et al., 2007). The intense band, centered at 1035 cm^{-1} , can be associated to the C–O stretching modes of hydroxyl and ether groups in cellulose (Paiva et al., 2007). The little peak at 892 cm^{-1} can be attributed to the presence of b-glycosidic linkages between the monosaccharides (De Rosa et al., 2010) whilst the absorbance at 598 cm^{-1} corresponds to the C–OH bending (Mwaikambo & Ansell, 2002).

3.5. Mechanical characterization

As reported for other lignocellulosic fibers (De Rosa et al., 2010; Fiore et al., 2011), arundo fibers show a brittle behavior with a sudden load drop when fiber failure happens (Fig. 6).

Three different parts can be distinguished in the stress–strain curve: a first linear part, until about 0.3% of deformation; a second non-linear part, which corresponds to strains from about 0.3% to about 0.6%; and the final linear part from the strain of about 0.6% and until the final failure of the fiber. The first part could be associated with a global loading of the fiber, through the deformation of each cell wall. The non-linear part is due to an elasto-visco-plastic deformation of the fiber, especially of the thickest cell wall (S2). This kind of deformation response is the result of the re-arrangement of the amorphous parts of the wall (mainly made of pectins and hemicelluloses), itself caused by the alignment of the cellulosic microfibrils with the tensile axis. The final linear part corresponds to the elastic response of the aligned microfibrils to the applied tensile strain (Charlet, Eve, Jerno, Gomina, & Breard, 2009). Let l_f be the length of a microfibril which initially forms an angle α with the fiber axis. The tension of the fiber brings about a change in the ori-

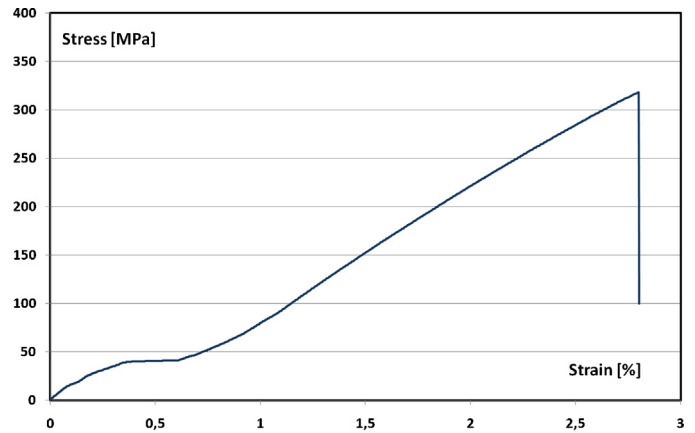


Fig. 6. Stress/strain curve of arundo fibers.

entation of the microfibrils and a corresponding fiber lengthening Δl :

$$\Delta l = l_f - l_0 = l_0 \cdot \left(\frac{1}{\cos \alpha} - 1 \right) \quad (3)$$

$$\varepsilon = \ln \cdot \left(1 + \frac{\Delta l}{l_0} \right) = -\ln(\cos \alpha) \quad (4)$$

where ε is the strain corresponding to the beginning of the final linear part of the stress–strain curves. It is well known that the results of the tensile tests on single lignocellulosic fiber are difficult to analyze since a high scatter is observed. This scatter can be mainly related to several factors as test parameters/conditions, area measurements and plant characteristics (i.e. the source and age of the plant, the processes of fiber extraction and the presence of defects) (Liu, Han, Huang, & Zhang, 2009). For these reasons, a statistical approach

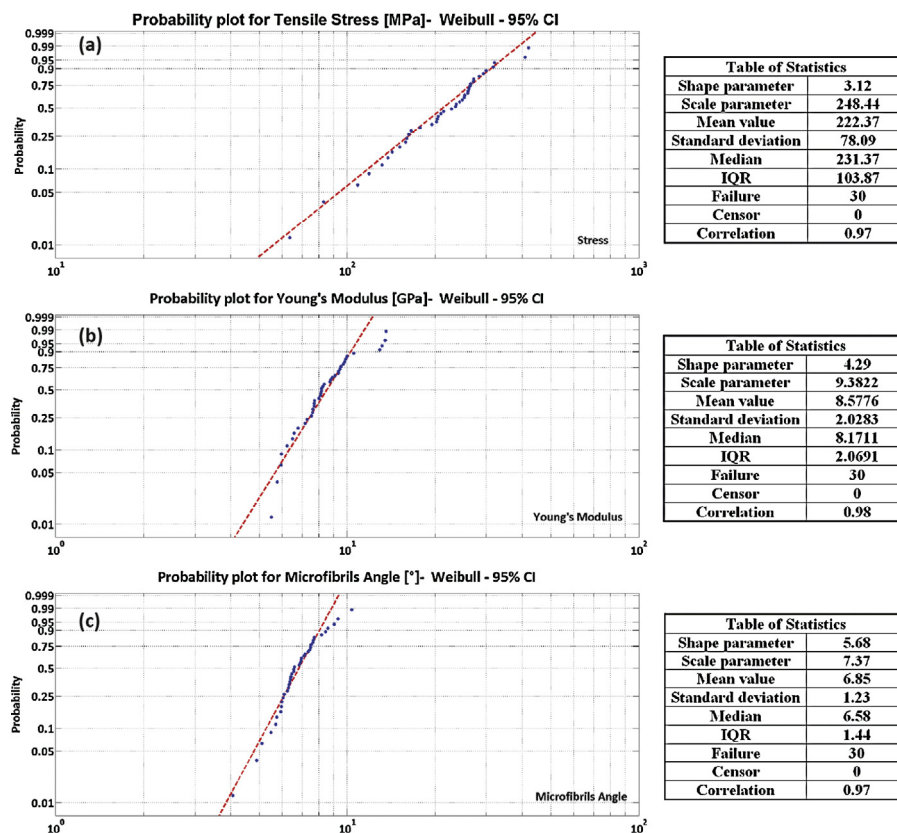


Fig. 7. Weibull distribution for (a) tensile stress, (b) Young's modulus and (c) microfibril angle of arundo fibers.

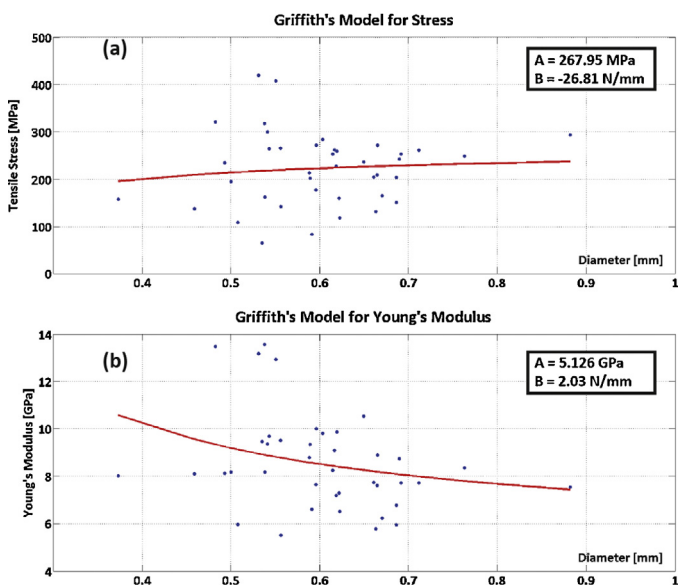


Fig. 8. Experimental data and Griffith model (line) for (a) tensile stress and (b) Young's modulus.

is required to evaluate the mechanical properties. The experimental data obtained by mechanical characterization were statistically analyzed using a two-parameter Weibull distribution, a method widely used to analyze mechanical and physical properties of lignocellulosic fibers (Andersons, Sparsinš, Joffe, & Wallström, 2005; De Rosa et al., 2010; Fiore et al., 2011; Weibull, 1939).

Fig. 7 shows the Weibull distributions for (a) tensile strength, (b) Young's modulus and (c) microfibril angle α calculated through Eq. (4) of arundo fibers. It can be seen that this model provides a good fitting of the data. In the same figure, the Weibull shape and scale parameters for the investigated property are reported. In particular, the shape parameter indicates the reliability of the data.

Weibull fitting was performed also for the elongation at break. For sake of conciseness, the Weibull distribution for elongation at break is not shown. The Weibull scale and shape parameters for this property are equal to 3.24% and 5.30, respectively.

As shown in Table 1, it is worth nothing that mechanical properties of arundo fibers are comparable to those of other natural fibers currently investigated as potential reinforcement in polymer matrix composites. Moreover, the microfibril angle of arundo fibers (i.e. 7.37°) is also comparable to the ones of other natural fibers as jute (8.1°), flax (5°), hemp (6.2°), prosopis juliflora (10.64°) and banana (11° – 12°), respectively (Kulkarni, Satyanarayana, Rohatgi, & Vijayan, 1983; Saravanakumar, Kumaravel, Nagarajan, Sudhakar, & Baskaran, 2013). Fig. 8 shows respectively (a) tensile strength and (b) Young's modulus as a function of diameter for arundo fibers. These figures point out the presence of a wide range of diameters and of a high dispersion of results.

The Griffith model, described by the following equation, was fitted to the experimental data (De Rosa et al., 2010; Fiore et al., 2011; Griffith, 1921; Peponi, Biagiotti, Torre, Kenny, & Mondragón, 2008):

$$P_f(d_f) = A + \frac{B}{d_f} \quad (5)$$

where $P_f(d_f)$ represents the measured property, A and B are parameters and d_f is the fiber diameter. The red lines represent the Griffith curve. The results show how a two-parameter model is not accurate enough to interpolate experimental data since the high scatter.

4. Conclusions

All the Mediterranean area and several zone in the world are potential land for planting *A. donax* and producing its derivatives. Even if this non-wood plant has application in preserving and reconsolidation of hydro-geological risk areas and several traditional usages in agriculture, its invasive and aggressive behavior causes disposal problems. In this paper the fibers extracted from the stems of *A. donax* L. were examined to evaluate the possibility of using them as reinforcement in polymer composites. The thermal behavior of arundo fibers was fully investigated through TGA and DTG curves. Mechanical properties of these fibers were assessed by single fiber tensile tests and the results were analyzed through a Weibull distribution. Microfibrils angle was estimate and statistically analyzed. The real density of the fibers was evaluated using a helium pycnometer. A fitting attempt in the study of the theoretical dependence of mechanical properties by the fiber geometry with the experimental data was made. Moreover, the fiber morphology was investigated by scanning electron microscopy (SEM) and Fourier transform infrared spectrometry (FTIR) was carried out to analyze the chemical structure of their components. The experimental results are comparable to those of other common natural fibers, confirming that these fibers represent a valid alternative to these ones as reinforcement in polymer composites. The future goal of this research work is to combine this kind of fibers with thermoset or thermoplastic polymers obtained from natural sources in order both to analyze the fiber/matrix adhesion, evaluating the necessity of a chemical pre-treatment of the fibers, and to study the mechanical properties of this new kind of composites. In conclusion, this non-wood plant could be cultivated and processed creating industrial chains who provide to extract fibers and to manufacture polymer composites with benefits in costs and for society and environment.

References

- Albano, C., Gonzalez, J., Ichazo, M., & Kaiser, D. (1999). Thermal stability of blends of polyolefins and sisal fiber. *Polymer Degradation and Stability*, 66, 179–190.
- Andersons, J., Sparsinš, E., Joffe, R., & Wallström, L. (2005). Strength distribution of elementary flax fibres. *Composites Science and Technology*, 65, 693–702.
- Arifuzzaman Khan, G. M., Shaheruzzaman, M., Rahman, M. H., Abdur Razzaque, S. M., Islam, M. S., & Alam, M. d. S. (2009). Surface modification of okra bast fiber and its physico-chemical characteristics. *Fibers and Polymers*, 10, 65–70.
- Arrakhiz, F. Z., Elachaby, M., Bouhfid, R., Vaudreuil, S., Essassi, M., & Qaiss, A. (2012). Mechanical and thermal properties of polypropylene reinforced with Alfa fiber under different chemical treatment. *Materials and Design*, 35, 318–322.
- Biagiotti, J., Puglia, D., Torre, L., Kenny, J. M., Arbelaiz, A., Cantero, G., et al. (2004). A systematic investigation on the influence of the chemical treatment of natural fibers on the properties of their polymer matrix composites. *Polymer Composites*, 25, 470–479.
- Bledzki, A. K., Reihmane, S., & Gassan, J. (1996). Properties and modification methods for vegetable fibers for natural fiber composites. *Journal of Applied Polymer Science*, 59, 1329–1336.
- Charlet, K., Eve, S., Jerno, J. P., Gomina, M., & Breard, J. (2009). Tensile deformation of a flax fiber. *Procedia Engineering*, 1, 233–236.
- d'Almeida, J. R. M., Aquino, R. C. M. P., & Monteiro, S. N. (2006). Tensile mechanical properties, morphological aspects and chemical characterization of piassava (*Attalea funifera*) fibers. *Composites Part A: Applied Science and Manufacturing*, 37, 1473–1479.
- da Silva Santos, R., de Souza, A. A., De Paoli, M. A., & de Souza, C. M. L. (2010). Cardanol-formaldehyde thermoset composites reinforced with buriti fibers: Preparation and characterization. *Composites Part A: Applied Science and Manufacturing*, 41, 1123–1129.
- Das, S., Saha, A. K., Choudhury, P. H., Basak, R. K., Mitra, B. C., Todd, T., et al. (2000). Effect of steam pretreatment of jute fiber on dimensional stability of jute composite. *Journal of Applied Polymer Science*, 76, 1652–1661.
- De Rosa, I. M., Kenny, J. M., Puglia, D., Santulli, C., & Sarasini, F. (2010). Morphological, thermal and mechanical characterization of okra (*Abelmoschus esculentus*) fibres as potential reinforcement in polymer composites. *Composites Science and Technology*, 70, 116–122.
- Di Bella, G., Fiore, V., & Valenza, A. (2012). Fiber reinforced composites. In Q. Cheng (Ed.), *Natural fiber-reinforced composites* (pp. 57–90). Hauppauge, NY: Nova Science Publishers.

- Fiore, V., Valenza, A., & Di Bella, G. (2011). Artichoke (*Cynara cardunculus* L.) fibres as potential reinforcement of composite structures. *Composites Science and Technology*, 71, 1138–1144.
- Flores, J. A., Pastor, J. J., Martinez-Gabaron, A., Gimeno-Blanes, F. J., & Rodriguez-Guisado, I. (2011). *Arundo donax* chipboard based on urea-formaldehyde resin using under 4 mm particles size meets the standard criteria for indoor use. *Industrial Crops and Products*, 34, 1538–1542.
- George, J., Sreekala, M. S., & Thomas, S. (2001). A review on interface modification and characterization of natural fiber reinforced plastic composites. *Polymer Engineering and Science*, 41, 1471–1485.
- Griffith, A. A. (1921). The phenomena of rupture and flow in solids. *Philosophical Transactions of the Royal Society of London: Series A*, 221, 163–198.
- Hornsby, P. R., Hinrichsen, E., & Tarverdi, K. (1997). Preparation and properties of polypropylene composites reinforced with wheat and flax straw fibres. *Journal of Materials Science*, 32, 443–449.
- John, K. J., & Anandjiwala, R. D. (2008). Recent developments in chemical modification and characterization of natural fiber-reinforced composites. *Polymer Composites*, 29, 187–207.
- Kalia, S., Kaith, B. S., & Kaur, I. (2009). Pretreatments of natural fibers and their application as reinforcing material in polymer composites—A review. *Polymer Engineering and Science*, 49, 1253–1272.
- Kulkarni, A. G., Satyanarayana, K. G., Rohatgi, P. K., & Vijayan, K. (1983). Mechanical properties of banana fibers (*Musa sapientum*). *Journal of Materials Science*, 18, 2290–2296.
- Le Troedec, M., Sedan, D., Peyratout, C., Bonnet, J., Smith, A., Guinebreiere, R., et al. (2008). Influence of various chemical treatments on the composition and structure of hemp fibres. *Composites Part A: Applied Science and Manufacturing*, 39, 514–522.
- Li, Y., Mai, Y. W., & Ye, L. (2000). Sisal fibre and its composites: A review of recent developments. *Composites Science and Technology*, 60, 2037–2055.
- Liu, D., Han, G., Huang, J. H., & Zhang, Y. (2009). Composition and structure study of natural *Nelumbo nucifera* fiber. *Carbohydrate Polymers*, 75, 39–43.
- Liu, W., Mohanty, K., Drzal, L. T., Askel, P., & Misra, M. (2004). Effects of alkali treatment on the structure, morphology of native grass fibers as reinforcements for polymer matrix composites. *Journal of Materials Science*, 39, 1051–1054.
- Mathew, L., Joseph, K. U., & Joseph, R. (2006). Isora fibre: Morphology, chemical composition, surface modification, physical, mechanical and thermal properties – A potential natural reinforcement. *Journal of Natural Fibers*, 3, 13–27.
- Meredith, R. (1956). *The mechanical properties of textile fibers*. Amsterdam: North-Holland Publishing Company.
- Mohanty, A. K., Misra, M., & Drzal, L. T. (2001). Surface modifications of natural fibers and performance of the resulting biocomposites: An overview. *Composite Interfaces*, 8, 313–343.
- Mwaikambo, L. Y., & Ansell, M. P. (2001). The determination of porosity and cellulose content of plant fibers by density methods. *Journal of Materials Science Letters*, 20, 2095–2096.
- Mwaikambo, L. Y., & Ansell, M. P. (2002). Chemical modification of hemp, sisal, jute, and kapok fibers by alkalization. *Journal of Applied Polymer Science*, 84, 2222–2234.
- Olsson, A. M., & Salmen, L. (2004). The association of water to cellulose and hemicellulose in paper examined by FTIR spectroscopy. *Carbohydrate Research*, 339, 813–818.
- Ouajai, S., & Shanks, R. A. (2005). Composition, structure and thermal degradation of hemp cellulose after chemical treatments. *Polymer Degradation and Stability*, 89, 327–335.
- Paiva, M. C., Ammar, I., Campos, A. R., Cheikh, R. B., & Cunha, A. M. (2007). Alfa fibres: Mechanical, morphological and interfacial characterization. *Composites Science and Technology*, 67, 1132–1138.
- Peponi, L., Biagiotti, J., Torre, L., Kenny, J. M., & Mondragón, I. (2008). Statistical analysis of the mechanical properties of natural fibers and their composite materials. I. Natural fibers. *Polymer Composites*, 29, 313–330.
- Pilu, R., Bucci, A., Badone, F., & Landoni, M. (2012). Giant reed (*Arundo donax* L.): A weed plant or a promising energy crop? *African Journal of Biotechnology*, 11, 9163–9174.
- Rong, M. Z., Zhang, M. Q., Liu, Y., Yang, G. C., & Zeng, H. M. (2001). The effect of fiber treatment on the mechanical properties of unidirectional sisal-reinforced epoxy composites. *Composites Science and Technology*, 61, 1437–1447.
- Saravanakumar, S. S., Kumaravel, A., Nagarajan, T., Sudhakar, P., & Baskaran, R. (2013). Characterization of a novel natural cellulosic fiber from *Prosopis juliflora* bark. *Carbohydrate Polymers*, 92, 1928–1933.
- Sarikanat, M., Seki, Y., Sever, K., & Durmuşkahya, C. (2014). Determination of properties of *Althaea officinalis* L. (Marshmallow) fibres as a potential plant fibre in polymeric composite materials. *Composites Part B: Engineering*, 57, 180–186.
- Sathishkumar, T. P., Navaneethakrishnan, P., Shankar, S., & Rajasekar, R. (2013). Characterization of new cellulose *sansevieria ehrenbergii* fibers for polymer composites. *Composite Interfaces*, 20, 575–593.
- Saura-Calixto, F., Cañellas, J., & Garcia-Raso, J. (1983). Determination of hemicellulose, cellulose and lignin contents of dietary fibre and crude fibre of several seed hulls. Data comparison. *Zeitschrift für Lebensmittel-Untersuchung und -Forschung*, 177, 200–202.
- Seki, Y., Sarikanat, M., Sever, K., & Durmuşkahya, C. (2013). Extraction and properties of *Ferula communis* (chakshir) fibers as novel reinforcement for composites materials. *Composites Part B: Engineering*, 44, 517–523.
- Sgriccia, N., Hawley, M. C., & Misra, M. (2008). Characterization of natural fiber surfaces and natural fiber composites. *Composites Part A: Applied Science and Manufacturing*, 39, 1632–1637.
- Silva, F. A., Chawla, N., & Toledo Filho, R. D. (2008). Tensile behavior of high performance natural (sisal) fibers. *Composites Science and Technology*, 68, 3438–3443.
- Ververis, C., Georghiou, K., Christodoulakis, N., Santas, P., & Santas, R. (2004). Fiber dimensions, lignin and cellulose content of various plant materials and their suitability for paper production. *Industrial Crops and Products*, 19, 245–254.
- Weibull, W. (1939). *A statistical theory of the strength of materials*. Stockholm: Ingeniörs Vetenskaps Akadem Handlingar.
- Yang, H., Yan, R., Chen, H., Lee, D. H., & Zheng, C. (2007). Characteristics of hemicellulose, cellulose and lignin pyrolysis. *Fuel*, 86, 1781–1788.
- Yao, F., Wu, Q., Lei, Y., Guo, W., & Xu, Y. (2008). Thermal decomposition kinetics of natural fibers: Activation energy with dynamic thermogravimetric analysis. *Polymer Degradation and Stability*, 93, 90–98.